This is the accepted manuscript of the article, which has been published in *Molecular Cancer Therapeutics*. 2019, 18(10), 1721-1730. https://doi.org/10.1158/1535-7163.MCT-19-0207

A Novel Anti-HER2 Antibody-Drug Conjugate XMT-1522 for HER2-Positive Breast And Gastric Cancers Resistant to Trastuzumab Emtansine

Vadim Le Joncour[1], Ana Martins[1], Maija Puhka[2], Jorma Isola[3], Marko Salmikangas[4], Pirjo Laakkonen[1,5*], Heikki Joensuu[1,4,6*], and Mark Barok[1,4*]

[1]Translational Cancer Medicine Research Program, Faculty of Medicine, University of Helsinki, Helsinki, Finland. [2]Institute for Molecular Medicine FIMM and EV Core, University of Helsinki, Helsinki, Finland. [3]Tampere University, Faculty of Medicine and Health Technology, Tampere, Finland. [4]Laboratory of Molecular Oncology, University of Helsinki, Biomedicum, Helsinki, Finland. [5]Laboratory Animal Center, Helsinki Institute of Life Science (HiLIFE), University of Helsinki, Helsinki, Finland. [6]Department of Oncology, Helsinki University Hospital and University of Helsinki, Helsinki, Finland.

[*]Equal contribution

Running title: XMT-1522 is Effective for T-DM1 Resistant Breast and Gastric Cancers

Grant Support

This study was supported by Academy of Finland, Cancer Society of Finland, Sigrid Juselius Foundation, Jane and Aatos Erkko Foundation, Helsinki University Research Grants, and a Mersana Therapeutics Inc. Grant.

Corresponding Author

Mark Barok, Laboratory of Molecular Oncology, Biomedicum Helsinki, Haartmaninkatu 8, Helsinki FIN-00290, Finland; Phone: +358-409345407; E-mail: mark.barok@helsinki.fi

Disclosure of Potential Conflicts of interest

MB received a personal grant from Mersana Therapeutics Inc.; HJ is a board member of Sartar Therapeutics, has a co-appointment at Orion Pharma, and has received fees from Orion Pharma and Neutron Therapeutics Ltd.

Word count: 4,381 (max. allowed: 5,000)

Figures: 6; Supplementary table: 1; Supplementary figures: 7

Key words

HER2, antibody-drug conjugate, breast cancer, gastric cancer, T-DM1, XMT-1522

Abstract

Most patients with HER2-positive breast or gastric cancer exhibit primary or acquired resistance to trastuzumab emtansine (T-DM1), and such patients may have limited therapeutic options. XMT-1522 is a novel anti-HER2 antibody-drug conjugate. We compared XMT-1522 to T-DM1 in preclinical models. The effects of XMT-1522 and T-DM1 on cell survival and apoptosis were compared in six HER2-positive breast cancer or gastric cancer cell lines, of which three lines were T-DM1-sensitive (N-87, OE-19, JIMT-1) and three T-DM1-resistant (RN-87, ROE-19, SNU-216). We compared these agents also in the HER2-negative breast cancer cell line MCF-7, and in mouse RN-87 and JIMT-1 xenograft models. Cell survival was assessed using the AlamarBlue method and apoptosis with the Caspase-Glo 3/7 method. XMT-1522 inhibited the growth of all six HER2-positive cell lines. The proportions of cells that survived XMT-1522 treatment were smaller as compared to T-DM1, particularly in the T-DM1-resistant cell lines. XMT-1522 induced more cell apoptosis compared to T-DM1. While RN-87 and JIMT-1 xenograft tumors progressed on T-DM1 treatment, all tumors responded to XMT-1522, and all but one tumor disappeared during the XMT-1522 treatment. XMT-1522 had a strong anti-tumor effect on RN-87 and JIMT-1 xenografts that progressed on T-DM1. We conclude that XMT-1522 was effective in HER2-positive breast cancer and gastric cancer cell lines resistant to T-DM1, and in xenograft models resistant to T-DM1. The results support the testing of XMT-1522 in clinical trials in patients with HER2-positive cancer.

Abstract word count: 233

Introduction

Overexpression and amplification of the human epidermal growth factor receptor-2 (HER2) is present in about 15-20% of human breast cancers and gastric cancers (1-3). Trastuzumab, a humanized monoclonal antibody that binds to the extracellular domain IV of HER2, has substantial anti-tumor activity, and is approved for the treatment of HER2-positive breast cancer and for HER2-positive metastatic gastric or gastroesophageal junction adenocarcinoma (4,5). Although responses to trastuzumab are often durable, most advanced cancers eventually become resistant to trastuzumab (6-8).

Antibody-drug conjugates (ADC) can deliver cytotoxic payloads to cancer cells. Trastuzumab emtansine (T-DM1, Kadcyla) is an anti-HER2 ADC where trastuzumab is linked with DM1 (a derivative of maytansine) via a non-reducible thioether linker (9). One T-DM1 carries an average of 3.5 DM1 moieties. DM1 and other T-DM1 catabolites such as MCC-DM1 (4-[N-maleimidomethyl]cyclohexane-1-carbonyl-DM1) and lysine-MCC-DM1 are released following receptor-mediated internalization and lysosomal degradation of the conjugate (10). Intracellular DM1 is a potent inhibitor of the microtubule assembly thereby causing cell death (9,11). The U.S. Food and Drug Administration (FDA) approved T-DM1 as monotherapy for the treatment of patients with HER2-positive advanced breast cancer who had previously received trastuzumab and a taxane in 2013 (12,13). As with trastuzumab, the majority of the initially responding advanced breast cancers eventually became resistant to T-DM1 (12,13). Adjuvant T-DM1 was superior to trastuzumab in a randomized trial in patients with HER2-positive breast cancer who had residual cancer in the breast or axilla at surgery after neoadjuvant chemotherapy and trastuzumab (14), but it was not superior to taxane chemotherapy in a patient population with previously treated HER2-positive advanced gastric cancer in a randomized trial (15).

XMT-1522 is a novel anti-HER2 ADC containing a human IgG1 anti-HER2 monoclonal antibody (HT-19) that binds to domain IV of HER2 to an epitope that is distinct from the trastuzumab binding site, and it does not compete with trastuzumab for HER2 binding. In XMT-1522, each antibody is armed with an average of 12 auristatin F-hydroxypropylamide (AF-HPA) moieties, linked to HT-19 via a cysteine linkage using a biodegradable hydrophilic polymer that enables high AF-HPA loading (16) (the structure of XMT-1522 is provided in the Supplement). Both AF-HPA and its intracellular catabolite auristatin F (AF) are potent inhibitors of tubulin polymerization (17).

We compared XMT-1522 to T-DM1 in both T-DM1-sensitive and T-DM1-resistant *in vitro* and *in vivo* models of breast cancer and gastric cancer, and found XMT-1522 to be in general more effective than T-DM1. To our knowledge, this is the first study to demonstrate that XMT-1522 has pronounced anti-cancer effect on HER2-positive T-DM1-resistant cancers.

Materials and methods

Cell lines

The cell lines used are summarized in Supplementary table 1. OE-19 was obtained from the European Collection of Cell Culture (CAMR Centre for Applied Microbiology and Research, Wiltshire, UK), NCI-N87 (N-87) and MCF-7 from the American Type Culture Collection (ATCC, Manassas, VA, USA), SNU-216 from the Korean Cell Line Bank (Seoul, Korea), and JIMT-1 from the laboratory of Cancer Biology, University of Tampere, Finland (18). The cell lines were cultured according to the recommended specifications.

We generated the T-DM1-resistant HER2-positive gastric cancer cell lines ROE-19 and RN-87 by treating OE-19 and N-87 cells, respectively, with increasing concentrations of T-DM1 (Roche Ltd., Basel, Switzerland). N-87 and OE-19 cells sensitive to T-DM1 were initially exposed to 0.12

µg/mL or 0.08 µg/mL of T-DM1, respectively, and then to gradually increasing concentrations of T-DM1 up to a maximum concentration of 2 µg/mL over 7 months (N-87) or 9 months (OE-19). Authentication of cell lines was performed using short tandem repeat analysis. All lines were tested for Mycoplasma routinely and only Mycoplasma-free cells were used.

In vitro assays of cell viability and caspase activation

The effects of T-DM1 and XMT-1522 (Mersana Therapeutics Inc., Cambridge, MA, USA) on the cell growth were studied using the AlamarBlue method (Thermo Fisher Scientific, Waltham, USA). The cells were trypsinized and plated in 96-well, flat-bottomed tissue culture plates. The effects of T-DM1 and XMT-1522 were tested at concentrations of 0.0001, 0.0006, 0.003, 0.016, 0.08, 0.4, 1, 2, and 10 µg/mL. The MCF-7 breast cancer cell line with low HER2 expression was used as the negative control. The numbers of viable cells were assessed after 5 days of incubation by addition of the AlamarBlue reagent (Thermo Fisher Scientific). Fluorescence was measured with excitation at 540 nm and emission at 590 nm using a PHERAstar FS plate reader (BMG Labtech, Germany). The fluorescence of the samples was normalized to the fluorescence of the cell-free culture media. The results are presented as the proportion of viable cells, obtained by dividing the fluorescence of the test samples by the fluorescence of the phosphate-buffered saline (PBS)-treated control samples. The dose achieving half-maximal (50%) inhibitory concentration (IC_{50}) with the drugs was calculated using the Graphpad Prism software (GraphPad Software, San Diego, USA).

To assess the rate of apoptosis, caspase activation was measured using the Caspase-Glo 3/7 method (Promega, Madison, USA) (19). The cells were trypsinised and plated in 96-well flat-bottomed tissue culture plates. After overnight culture, the medium was exchanged to a medium containing 0.0006, 0.003, 0.016, 0.08, 0.4, 1, or 2 µg/mL concentration of either T-DM1 or XMT-1522. After 48 hours of incubation, 100 µL of the medium was transferred into white-walled 96-well plates, mixed with 100 µL Caspase-Glo 3/7 reagent, incubated for 30 min at RT, and the luminescence was

recorded using a PHERAstar FS plate reader (BMG Labtech). The results are presented as luminescence units obtained after subtracting the luminescence value from a blank reaction (without T-DM1 or XMT-1522 treatment).

Mouse xenografts

The National Animal Experiment Board of Finland approved the mouse experiments. Five to 8-week-old female SCID mice (Envigo RMS B.V., Horst, The Netherlands) were injected subcutaneously with 15×10^6 or 18×10^6 of human breast cancer cells (JIMT-1) in 150 μL of the culture medium (DMEM supplemented with 10% FBS), 14×10^6 of human gastric cancer cells (N-87), or with 25×10^6 of T-DM1-resistant human gastric cancer cells (RN-87) in 150 μL of the cell culture medium (RPMI supplemented with 10% FBS) to establish xenograft tumors. Following this, T-DM1 (5 mg/kg) or XMT-1522 (1 mg/kg or 3 mg/kg) were administered intravenously (i.v.) at 7-day intervals. As a control, PBS was administered intraperitoneally (i.p.) at 7-day intervals. Tumor size was measured using a caliper, and tumor volume was calculated using the formula $T_{vol} = \pi/6 \times$ larger diameter $\times$ (smaller diameter)^2. Mice with tumor > 20 mm in any one dimension or tumor ulceration were sacrificed using CO_2 inhalations and cervical dislocations.

Electron microscopy

Extracellular vesicle (EV) samples were prepared for electron microscopy and imaged as described elsewhere (19,20) using an immunostaining procedure. In brief, after paraformaldehyde fixation, the samples were blocked with 0.5% bovine serum albumin (BSA) in 0.1 M sodium phosphate buffer (pH 7.0) for 10 min at RT, incubated with a 12 nm colloidal gold-conjugated goat-anti-human-IgG secondary antibody (gold-GAHIG; Jackson ImmunoResearch) in the same sodium phosphate buffer for 30 min at RT, washed with the sodium phosphate buffer and deionized water, stained with uranyl acetate, and embedded in a methyl cellulose uranyl acetate mixture. The samples were viewed using either a Tecnai 12 transmission electron microscope (FEI Company,

Eindhoven, The Netherlands) or a Jeol JEM-1400 transmission electron microscope (Jeol Ltd., Tokyo, Japan,), each operating at 80 kV.

Other methods

The methods used for RNA isolation, RNA expression analysis, immunohistochemistry, fluorescence *in situ* hybridization, flow cytometry, EV sample preparation and analysis, and the nanoparticle tracking analysis are provided in the Supplement.

Statistical analysis

Data are expressed as the mean ± SE. Groups were compared using Student's t test when the data passed the normality test. Gene expression data were compared using two-way ANOVA. Unpaired groups were compared with the Mann-Whitney test. Survival was analyzed using the Kaplan-Meier method, and survival between groups was compared with the log-rank test. Statistical calculations were carried out using the IBM SPSS version 24 (IBM, Armonk, USA). All *P* values are two-sided.

Results

XMT-1522 inhibits the growth of T-DM1-resistant cells *in vitro*

The growth inhibitory effects of T-DM1 and XMT-1522 were compared in six HER2-positive cancer cell lines and in the control cell line (MCF-7) that does not harbor *HER2* amplification and has a low level of HER2 protein expression (21). XMT-1522 inhibited the growth of all HER2-positive cell lines in a dose-dependent manner. The proportion of cells surviving the treatments was smaller with XMT-1522 than with T-DM1 particularly in the ROE-19, RN-87, and SNU-216 gastric cancer cell lines that are resistant to T-DM1. The 50% inhibitory concentration (IC_{50}) was achieved with XMT-1522 in all six HER2-positive cell lines, but with T-DM1 only in the OE-19, N-87, and JIMT-1 cell lines, where XMT-1522 yielded 2.5-fold (OE-19), 3.6-fold (N-87), and 13-

fold (JIMT-1) greater growth inhibition as compared with T-DM1. The IC_{50} values of XMT-1522 on N-87 and RN-87 cell lines (0.010 and 0.011 µg/mL, respectively) and OE-19 and ROE-19 cell lines (0.008 and 0.011 µg/mL, respectively) were similar, suggesting similar activity of XMT-1522 in the parent cell line and the corresponding T-DM1-resistant derivative cell line. As expected, neither T-DM1 nor XMT-1522 was effective in the HER2-negative MCF-7 cell line (Fig. 1, A-G).

To estimate the rate of apoptosis, we studied the influence of T-DM1 and XMT-1522 on caspase-3 and/or caspase-7 in the HER2-positive cell lines JIMT-1 and RN-87. In both cell lines XMT-1522 increased caspase-3 and/or caspase-7 activity in a dose-dependent manner more than T-DM1 (Fig. 1, H & I).

XMT-1522 eradicates T-DM1-resistant RN-87 xenografts *in vivo*

The effects of XMT-1522 and T-DM1 on the growth of RN-87 xenografts was compared in mice. The RN-87 gastric cancer xenografts expressed HER2 at the same level as the T-DM1-sensitive parental N-87 xenografts (Supplementary Fig. 1, A & B). Tumors formed in all 44 mice inoculated with RN-87 cell suspension within 7 days from the date of inoculation reaching a mean tumor volume of 39.5 ± 11.4 mm^3 on day 7. On day 18 since inoculation, the mice were split into four groups, and were treated weekly with either PBS (n = 12), T-DM1 5 mg/kg (n = 20), XMT-1522 1 mg/kg (n = 6), or XMT-1522 3 mg/kg (n = 6). T-DM1 did not inhibit tumor growth, whereas both doses of XMT-1522 induced rapid and complete tumor shrinkage (Fig. 2, A & B). Six out of the 20 T-DM1-treated mice were euthanized due to the presence of a large ulcerated tumor by day 35 since the inoculation, the T-DM1 treatment of nine mice was discontinued on day 35, and five mice continued to receive the T-DM1 treatment. From day 35 onwards four of the nine mice whose T-DM1 treatment was discontinued were treated with 1 mg/kg of XMT-1522 and five mice with 3 mg/kg of XMT-1522. All nine mice treated with XMT-1522 following the T-DM1 treatment had tumor shrinkage, whereas the five mice that continued on T-DM1 showed persistent tumor growth.

Two out of the five mice treated with 3 mg/kg of XMT-1522 were euthanized due to ulceration of the tumor on day 43 since the inoculation, and the three remaining mice had unmeasurable tumor by day 67. All four tumors treated with 1 mg/kg of XMT-1522 became unmeasurable by day 71. XMT-1522 treatment was discontinued for all the remaining animals on day 63 with follow-up until day 85. No tumor relapse was observed during the follow-up time. No significant difference in the tumor growth rate was observed between the two XMT-1522 dosing groups.

On day 35 since the date of tumor inoculation three out of the 12 mice allocated to PBS were switched to 1 mg/kg of XMT-1522, three to 3 mg/kg of XMT-1522, and three to 5 mg/kg of T-DM1. The three remaining mice in the PBS group were euthanized due to large ulcerated tumors by day 35. The mice treated with T-DM1 had further cancer progression. In contrast, all six mice treated with XMT-1522 showed tumor shrinkage. One mouse from the 1 mg/kg XMT-1522 treatment group and one from the 3 mg/kg group were euthanized due to ulceration of the tumor on day 43 and on day 46 since the inoculation, respectively, but the four remaining tumors became unmeasurable by day 71 in the 1 mg/kg group and by day 67 in the 3 mg/kg group similar to the mice that were switched from T-DM1 to XMT-1522.

XMT-1522 increased mice survival compared to T-DM1 ($P < 0.001$; Supplementary Fig. 2A). The mice whose T-DM1 treatment was switched to XMT-1522 survived longer than the mice that had been treated continuously with T-DM1 ($P = 0.010$; Supplementary Fig. 2, B).

XMT-1522 eliminates breast cancer xenografts

The effects of XMT-1522 and T-DM1 were next compared using a JIMT-1 HER2-positive breast cancer xenograft model. Tumors formed in all 32 mice inoculated with the JIMT-1 cell suspension by day 7 with a mean tumor volume of 80.6 ± 26.9 mm^3 on day 7. On day 15 after the inoculation, the mice were split into four treatment groups, and were treated weekly for 3 weeks with either PBS

(n = 10), T-DM1 (5 mg/kg, n = 10), XMT-1522 1 mg/kg (n = 6), or XMT-1522 3 mg/kg (n = 6). While the T-DM1-treated tumors grew continuously, tumor shrinkage was rapid in both XMT-1522 dosing groups. All six mice treated with 3 mg/kg of XMT-1522 and five out of the six mice treated with 1 mg/kg of XMT-1522 had no palpable tumor from day 70 onwards. The one remaining tumor shrunk from the size of 301.4 mm^3 on day 15 when XMT-1522 treatment was started to 4.2 mm^3 on day 63, and then started to grow reaching 14.1 mm^3 on day 98. From day 99 onwards this mouse was treated with XMT-1522 3 mg/kg for three weeks, which resulted in tumor shrinkage to 1.5 mm^3 on day 131. Mice allocated to XMT-1522 survived longer than those allocated to T-DM1 ($P < 0.001$; Fig. 3).

Next, the XMT-1522 and T-DM1 treatments were started at the time of JIMT-1 cell inoculation to compare the drug effects on tumor formation. Six mice treated with PBS were used as a control. The tumors in the T-DM1-treated mice (n = 18) remained small until day 27, but then started to grow. In the two XMT-1522 dosing groups (1 mg/kg and 3 mg/kg, n = 6 each) no tumors were detectable from day 20 onwards (Fig. 4, A & B). The mice treated with T-DM1 survived longer than the control group mice ($P < 0.001$) while the mice allocated to XMT-1522 survived longer than those treated with T-DM1 ($P < 0.001$; Fig. 4, C).

XMT-1522 was also tested in mice that had cancer progression while on T-DM1 5 mg/kg weekly. Two of these 18 mice were euthanized due to a large ulcerated tumor by day 43 since the date of tumor inoculation. On day 43, ten of the remaining 16 mice had the treatment switched to either 1 mg/kg of XMT-1522 (n = 5) or 3 mg/kg of XMT-1522 (n = 5), and 6 mice continued with T-DM1 treatment. The tumors of the 6 mice that continued with T-DM1 treatment progressed, while the mice treated with XMT-1522 had rapid tumor shrinkage irrespective of the XMT-1522 dosage (Fig. 4, A & B). Four out of the 5 mice treated with XMT-1522 3 mg/kg had no palpable tumor from day 76 onwards, but one tumor became detectable on day 125 and then progressed. Two out of the 5

mice treated with XMT-1522 1 mg/kg had no palpable tumor from day 83 onwards, the 3 remaining tumors first shrank (to unmeasurable, 14.1 mm^3, and 6.3 mm^3), but then started to regrow and continued to progress despite administration of the 3 mg/kg dose of XMT-1522. The mice that had T-DM1 switched to XMT-1522 survived longer than the mice that continued with T-DM1 ($P < 0.001$; Fig. 4, D).

XMT-1522 evokes apoptosis in T-DM1-resistant breast cancer and gastric cancer xenografts

More apoptotic cells were detected in the RN-87 and JIMT-1 xenografts treated with XMT-1522 than in tumors treated with T-DM1 (Fig. 5, A-D; Supplementary Fig. 3). A higher number of apoptotic cells was present in the JIMT-1 tumor that relapsed after being treated with the 1 mg/kg dose of XMT-1522 but was still sensitive to the higher dose (Fig. 5, E), whereas only few apoptotic cells were observed in the JIMT-1 tumors that grew during XMT-1522 treatment (Fig 5, F).

Expression of HER2 and EGFR on T-DM1-treated and XMT-1522-treated JIMT-1 xenografts

JIMT-1 tumors treated continuously with T-DM1 retained their HER2 expression, but gained some EGFR expression (Supplementary Fig. 4, A-B, F-G). The JIMT-1 tumor that ceased to respond to 1 mg/kg of XMT-1522 but responded to 3 mg/kg of XMT-1522 remained HER2-positive and EGFR-negative (Supplementary Fig. 4, D & I). All 4 tumors that progressed on T-DM1 and were subsequently treated with XMT-1522 and after an initial response progressed also on XMT-1522 had lost the HER2 expression, and two of the four progressing tumors expressed slightly also EGFR (Supplementary Fig. 4, E & J). Giant multinucleated cells and cells with aberrant mitotic morphology, the hallmarks of mitotic catastrophe (22), were observed in both T-DM1-treated and XMT-1522-treated xenografts (Supplementary Fig. 4, B-D, G-J).

Loss of *HER2* amplification in T-DM1-pretreated JIMT-1 xenografts that progressed on XMT-1522 treatment

Interestingly, JIMT-1 tumors that progressed on T-DM1 and were subsequently treated with XMT-1522 and that after an initial response progressed also on XMT-1522 showed loss of *HER2* gene amplification unlike JIMT-1 tumors that were continuously treated with T-DM1 ($P < 0.0001$; Supplementary Fig. 5, A-D).

***HER2* and ATP-binding cassette (ABC) transporter mRNA and protein expression in the T-DM1-resistant cell lines**

To elucidate the mechanisms associated with the T-DM1 resistance, gene expression of the T-DM1-sensitive parental gastric cancer cell lines (N-87, OE-19) was compared to their resistant counterparts (RN-87, ROE-19). Slight down-regulation of *HER2* mRNA was detected in the resistant cells as compared to the corresponding sensitive cell lines (RN-87 vs. N-87, 1.35-fold decrease; ROE-19 vs. OE-19, 1.72-fold decrease). ATP-binding cassette (ABC) transporters may cause resistance to anticancer therapy by increasing the efflux of chemotherapy agents from cancer cells (23). Substantial upregulation of *ABCC2* and *ABCG2* mRNA was found in the resistant RN-87 cells as compared to the sensitive N-87 cells (1385-fold and 116-fold increase, respectively), and significant upregulation of *ABCC1* and *ABCC2* was detected in the resistant ROE-19 cells as compared to the sensitive OE-19 cells (98-fold and 37-fold increase, respectively) (Fig. 6, A).

Flow cytometric analyses of the corresponding protein levels supported these findings. Resistant RN-87 and ROE-19 cells had lower cell surface HER2 expression than the sensitive N-87 cells and OE-19 cells ($P = 0.005$ and $P = 0.007$, respectively; Fig. 6, B). There were no significant associations between the drug responses (IC_{50} values) to either T-DM1 or XMT-1522 and the numbers of cell surface HER2 receptors ($r = -0.94$, $P = 0.23$; $r = -0.49$, $P = 0.32$, respectively) (Fig. 6, C). The expression of ABCC1, ABCC2, and ABCG2 proteins in the cell lines were in agreement

with the corresponding mRNA expression levels. SNU-216 gastric cancer cells had very low levels of ABCC1 and ABCG2 (Fig. 6, D-F).

Inhibition of ABC transporters sensitizes the resistant cells to T-DM1

To investigate the role of ABC transporters in resistance to T-DM1, three ABC transporter inhibitors tetrandrine, MK571, and elacridar were studied either as single agents or in a combination with T-DM1 in HER2-positive T-DM1-resistant gastric cancer cell lines RN-87 and ROE-19. MK571 (Sigma-Aldrich) is an inhibitor of ABCC1, ABCC2, and ABCG2 (24,25), elacridar (Sigma-Aldrich) inhibits ABCB1 and ABCG2 (26), and tetrandrine (Abcam, Cambridge, UK) inhibits ABCB1 and ABCC1 (27). Tetrandrine (5 µM), MK571 (50 µM), and elacridar (1 µM) were used either alone or combined with T-DM1 at concentrations of 10 µg/mL, 10 µg/mL, and 2 µg/mL, respectively. In each experiment, the combination of an ABC transporter inhibitor and T-DM1 resulted in the lowest cell survival (Fig. 6, G-I). These data suggest that overexpression of ABCC1, ABCC2, and ABCG2 transporters decreases biological activity of T-DM1 in RN-87 and ROE-19 cells.

T-DM1-resistant cells dispose T-DM1 by extracellular vesicle (EV) secretion

Cancer cells can dispose T-DM1 by EV secretion (19), and we, therefore, compared this mechanism between the T-DM1-sensitive N-87 and T-DM1-resistant RN-87 cells. EVs of 30 to 300 nm in diameter were detected by using transmission electron microscopy and no difference in the EV particle size distributions were detected between the two cell lines by nanoparticle tracking analysis (Supplementary Fig. 6). At immuno-electron microscopy, T-DM1 was present on the surface of EVs derived from both N-87 and RN-87 cells treated with T-DM1 (Supplementary Fig. 7, A & B). Higher amounts of T-DM1 were found on the EVs prepared from RN-87 cells than on those derived from N-87 ($P = 0.036$) in a flow cytometry analysis suggesting that the resistant cells dispose more T-DM1 by secreting EVs than the T-DM1-sensitive cells. The T-DM1 binding capacity (TBC) of

the EVs harvested from the RN-87 cells was also higher than that of the EVs harvested from N-87 cells ($P = 0.037$; Supplementary Fig. 7, C & D).

Discussion

Most cancers treated with T-DM1 eventually progress (12,13), and, therefore, novel agents for treating T-DM1-resistant HER2-positive cancers are needed. We report here that both breast and gastric cancer cells resistant to T-DM1 are sensitive to XMT-1522, a next generation anti-HER2 ADC. XMT-1522 had a more pronounced growth inhibitory effect on breast and gastric cancer cells sensitive to T-DM1 than T-DM1 *in vitro*, and XMT-1522 had marked anti-cancer efficacy *in vitro* and in mouse xenograft models of breast cancer and gastric cancer with resistance to T-DM1.

The biological activity of T-DM1 likely depends on the cytosolic concentration of its cytotoxic moiety, DM1. Therefore, the factors that decrease the intracellular DM1 concentration may contribute to resistance (11), such as decreased expression of HER2 leading to delivery of less T-DM1 into the cells (28), and overexpression of drug efflux proteins that can discard DM1 from the cells (24,28). In line with these observations, we detected decreased expression of HER2 on the T-DM1-resistant RN-87 and ROE-19 gastric cancer cells as compared to their sensitive parental cells. In addition, the resistant cells expressed higher levels of ABCC1 (multi-drug resistance protein 1), ABCC2 (multi-drug resistance protein 2), and ABCG2 (breast cancer resistance protein). Inhibitors of these transporters (MK571, elacridar, and tetrandrine) restored the sensitivity of the resistant cells to T-DM1, suggesting that these transporters play a role in the T-DM1 resistance in RN-87 and ROE-19 cells. We also propose a novel mechanism that can further decrease intracellular DM1 concentrations. When we compared T-DM1-sensitive and T-DM1-resistant cancer cells (N-87 and RN-87, respectively), the secreted extracellular vesicles (EV) derived from the resistant cells

contained more HER2 compared to the EVs derived from the sensitive cells (although the resistant cells had less cell surface HER2), and more T-DM1 was present on EVs harvested from the T-DM1-resistant RN-87 cells. Therefore, disposal of T-DM1 on the secreted EVs by the resistant cells may contribute to T-DM1 resistance.

Loss of HER2 expression and increased EGFR expression were linked to the acquired T-DM1 resistance based on an *in vitro* JIMT-1 breast cancer cell model (29). We found decreased, but still substantial expression of HER2 protein in the T-DM1-resistant JIMT-1 xenografts, and increased expression of EGFR. While higher EGFR expression could serve as a growth signal bypassing HER2, the mechanisms causing T-DM1 resistance in JIMT-1 cells remain largely unknown.

We tested three strategies to administer XMT-1522 in mouse xenograft models, and found XMT-1522 effective in each setting. When XMT-1522 was administered to mice carrying small subcutaneous tumors that had not been treated previously, all RN-87 gastric cancer xenografts and all but one JIMT-1 breast xenograft shrank rapidly and disappeared. XMT-1522 was also effective on larger xenograft tumors that were resistant to T-DM1. In this setting, most RN-87 gastric cancer xenografts and most JIMT-1 breast cancer xenografts disappeared during the XMT-1522 treatment. Interestingly, several of the few tumors that did not regress completely on XMT-1522 treatment or recurred following XMT-1522 treatment were HER2-negative in both immunohistochemistry and FISH, suggesting that loss of HER2 expression, which might be caused by loss of *HER2* amplification, is a resistance mechanism to XMT-1522. In the third setting where drug administration was started already at the time of tumor cell inoculation mimicking micrometastatic disease and the adjuvant setting, XMT-1522 inhibited tumor formation, whereas in the T-DM1-treated mice the tumors progressed.

Retrospective analyses of two phase II trials evaluating T-DM1 showed lower response rates in patients with lower HER2 levels (30,31), suggesting that response to T-DM1 depends on the amount of tumor HER2 expression even in the subset of cancers that were judged as HER2-positive. Hypothetically, high response rates may be achieved with ADCs that have a high drug antibody ratio (DAR). In XMT-1522 the cytotoxic AF-HPA moieties are conjugated to an anti-HER2 antibody via a polymer linker that allows high drug loading (16). The higher DAR of XMT-1522 compared to T-DM1 (12 vs. 3.5, respectively) may in part explain the superior anti-cancer efficacy of XMT-1522 in our breast and gastric cancer models as compared to T-DM1. Further study is needed to find out whether AF-HPA and its catabolite auristatin F (AF) are less avid substrates for the ABCC1, ABCC2, and ABCG2 transporters than lysine-MCC-DM1, the active catabolite of DM1.

The greater anti-cancer effect of XMT-1522 might also be related to the bystander effect. AF-HPA is membrane-permeable and can, therefore, enter the neighboring cells where AF-HPA is converted to highly cytotoxic but non-cell membrane permeable AF, which is trapped in the cells (17). In contrast, lysine-MCC-DM1 that is formed at proteolytic degradation of T-DM1 in the lysosomes cannot cross the cell membranes, and, therefore, T-DM1 lacks the bystander effect (9). Both DM1 and auristatins are highly cytotoxic payloads causing cell death by inhibiting tubulin polymerization (31). Antibody-dependent cellular cytotoxicity (ADCC) likely contributes substantially to the efficacy of trastuzumab and T-DM1 *in vivo* (22,32). HT-19, the antibody part of XMT-1522, may also evoke ADCC (33).

In summary, XMT-1522, an anti-HER2 ADC showed a stronger inhibitory effect on breast and gastric cancer cells sensitive to T-DM1 than T-DM1. In addition, it was efficacious on gastric cancer cells with primary or acquired resistance to T-DM1 *in vitro,* and XMT-1522 had anti-cancer efficacy also in T-DM1-resistant breast cancer and gastric cancer xenografts *in vivo*. The results

support clinical evaluation of XMT-1522 in patients with HER2-posive breast cancer or gastric cancer.

Authors' Contributions

VLJ discussed the hypothesis, designed the experimental approach, performed the experimental work, and participated in writing the manuscript.

AM discussed the hypothesis, designed the experimental approach, and performed the experimental work.

MP discussed the hypothesis, did electron microscopy, analyzed the data, contributed to the data interpretation and discussion.

JI discussed the hypothesis, designed the experimental approach, performed the experimental work, and interpreted data.

MS discussed the hypothesis, designed the experimental approach, performed the experimental work.

PL discussed the hypothesis and designed the experimental approach, interpreted data, and participated in writing the manuscript.

HJ led the project, discussed the hypothesis, designed the experimental approach, interpreted data, and drafted the manuscript together with MB.

MB conceived the hypothesis, led the project, designed the experimental approach, performed the experimental work, analyzed data, coordinated the project, and drafted the manuscript. All authors read and approved the final manuscript.

Acknowledgements

We thank Mersana Therapeutics Inc. for providing XMT-1522. We thank technician Mrs. Ben-Ami Marja for skillful help in performing the experiments, the Extracellular Vesicle Core

Facility at the University of Helsinki, Finland, for the electron microscopy work and for providing nanoparticle tracking analysis service, and the Electron Microscopy Unit of the Institute of Biotechnology, University of Helsinki for providing the facilities.

References

1. Slamon D, Clark G, Wong S, Levin W, Ullrich A, McGuire W. Human breast cancer: correlation of relapse and survival with amplification of the HER-2/neu oncogene. Science 1987;**235**:177-82.
2. Slamon D, Godolphin W, Jones L, Holt J, Wong S, Keith D, et al. Studies of the HER-2/neu proto-oncogene in human breast and ovarian cancer. Science 1989;**244**:707-12.
3. Gravalos C, Jimeno A. HER2 in gastric cancer: a new prognostic factor and a novel therapeutic target. Ann Oncol 2008;**19**:1523-9.
4. Slamon D, Leyland-Jones B, Shak S, Fuchs H, Paton V, Bajamonde A, et al. Use of chemotherapy plus a monoclonal antibody against HER2 for metastatic breast cancer that overexpresses HER2. N Engl J Med 2001;**344**:783-92.
5. Bang YJ, Van Cutsem E, Feyereislova A, Chung HC, Shen L, Sawaki A, et al. Trastuzumab in combination with chemotherapy versus chemotherapy alone for treatment of HER2-positive advanced gastric or gastro-oesophageal junction cancer (ToGA): a phase 3, open-label, randomised controlled trial. Lancet 2010;**376**:687-97.
6. Nahta R, Yu D, Hung M, Hortobagyi G, Esteva F. Mechanisms of disease: understanding resistance to HER2-targeted therapy in human breast cancer. Nat Clin Pract Oncol 2006;**3**:269-80.
7. Okines AF, Cunningham D. Trastuzumab: a novel standard option for patients with HER-2-positive advanced gastric or gastro-oesophageal junction cancer. Therap Adv Gastroenterol 2012;**5**:301-18.
8. Nahta R, Esteva FJ. HER2 therapy: molecular mechanisms of trastuzumab resistance. Breast Cancer Res 2006;**8**:215.
9. Lewis Phillips GD, Li G, Dugger DL, Crocker LM, Parsons KL, Mai E, et al. Targeting HER2-positive breast cancer with trastuzumab-DM1, an antibody-cytotoxic drug conjugate. Cancer Research 2008;**68**:9280-90.
10. Liu Y, Zhou F, Sang H, Ye H, Chen Q, Yao L, et al. LC-MS/MS method for the simultaneous determination of Lys-MCC-DM1, MCC-DM1 and DM1 as potential intracellular catabolites of the antibody-drug conjugate trastuzumab emtansine (T-DM1). J Pharm Biomed Anal 2017;**137**:170-7.
11. Barok M, Joensuu H, Isola J. Trastuzumab emtansine: mechanisms of action and drug resistance. Breast Cancer Res 2014;**16**:209.
12. Hurvitz SA, Dirix L, Kocsis J, Bianchi GV, Lu J, Vinholes J, et al. Phase II randomized study of trastuzumab emtansine versus trastuzumab plus docetaxel in patients with human epidermal growth factor receptor 2-positive metastatic breast cancer. J Clin Oncol 2013;**31**:1157-63.
13. Verma S, Miles D, Gianni L, Krop I, Welslau M, Baselga J, et al. Trastuzumab emtansine for HER2-positive advanced breast cancer. N Engl J Med 2012;**367**:1783-91.
14. von Minckwitz G, Huang CS, Mano MS, Loibl S, Mamounas EP, Untch M, et al. Trastuzumab Emtansine for Residual Invasive HER2-Positive Breast Cancer. N Engl J Med 2019;**380**:617-28.
15. Thuss-Patience PC, Shah MA, Ohtsu A, Van Cutsem E, Ajani JA, Castro H, et al. Trastuzumab emtansine versus taxane use for previously treated HER2-positive locally advanced or metastatic gastric or gastro-oesophageal junction adenocarcinoma (GATSBY): an international randomised, open-label, adaptive, phase 2/3 study. Lancet Oncol 2017;**18**:640-53.
16. Hamilton EP, Barve MA, Bardia A, Beeram M, Bendell JC, Mosher R, et al. Phase 1 dose escalation of XMT-1522, a novel HER2-targeting antibody-drug conjugate, in patients with HER2-expressing breast, lung and gastric tumors. J Clin Oncol 2018;**36**(Suppl) (abstract 2546).
17. Clardy SM, Yurkovetskiy A, Yin M, Gumerov D, Xu L, Ter-Ovanesyan E, et al. Unique pharmacologic properties of Dolaflexin-based ADCs - a controlled bystander effect. Cancer Res 2018;**78**(13 Suppl) (abstract 754).
18. Tanner M, Kapanen A, Junttila T, Raheem O, Grenman S, Elo J, et al. Characterization of a novel cell line established from a patient with Herceptin-resistant breast cancer. Mol Cancer Ther 2004;**3**:1585-92.
19. Barok M, Puhka M, Vereb G, Szollosi J, Isola J, Joensuu H. Cancer-derived exosomes from HER2-positive cancer cells carry trastuzumab-emtansine into cancer cells leading to growth inhibition and caspase activation. BMC Cancer 2018;**18**:504.

20. Puhka M, Nordberg ME, Valkonen S, Rannikko A, Kallioniemi O, Siljander P, et al. KeepEX, a simple dilution protocol for improving extracellular vesicle yields from urine. Eur J Pharm Sci 2017;**98**:30-9.
21. Barok M, Tanner M, Koninki K, Isola J. Trastuzumab-DM1 is highly effective in preclinical models of HER2-positive gastric cancer. Cancer Lett 2011;**306**:171-9.
22. Barok M, Tanner M, Koninki K, Isola J. Trastuzumab-DM1 causes tumour growth inhibition by mitotic catastrophe in trastuzumab-resistant breast cancer cells in vivo. Breast Cancer Res 2011;**13**:R46.
23. Leonard G, Fojo T, Bates S. The role of ABC transporters in clinical practice. Oncologist 2003;**8**:411-24.
24. Takegawa N, Nonagase Y, Yonesaka K, Sakai K, Maenishi O, Ogitani Y, et al. DS-8201a, a new HER2-targeting antibody-drug conjugate incorporating a novel DNA topoisomerase I inhibitor, overcomes HER2-positive gastric cancer T-DM1 resistance. Int J Cancer 2017;**141**:1682-9.
25. Koley D, Bard AJ. Inhibition of the MRP1-mediated transport of the menadione-glutathione conjugate (thiodione) in HeLa cells as studied by SECM. Proc Natl Acad Sci U S A 2012;**109**:11522-7.
26. Robey RW, Ierano C, Zhan Z, Bates SE. The challenge of exploiting ABCG2 in the clinic. Curr Pharm Biotechnol 2011;**12:**595-608.
27. Fanelli M, Hattinger CM, Vella S, Tavanti E, Michelacci F, Gudeman B, et al. Targeting ABCB1 and ABCC1 with their Specific Inhibitor CBT-1(R) can Overcome Drug Resistance in Osteosarcoma. Curr Cancer Drug Targets 2016;**16**:261-74.
28. Li G, Guo J, Shen BQ, Yadav DB, Sliwkowski MX, Crocker LM, et al. Mechanisms of Acquired Resistance to Trastuzumab Emtansine in Breast Cancer Cells. Mol Cancer Ther 2018;**17**:1441-53.
29. Endo Y, Shen Y, Youssef LA, Mohan N, Wu WJ. T-DM1-resistant cells gain high invasive activity via EGFR and integrin cooperated pathways. MAbs 2018;**10**:1003-17.
30. LoRusso P, Weiss D, Guardino E, Girish S, Sliwkowski M. Trastuzumab emtansine: a unique antibody-drug conjugate in development for human epidermal growth factor receptor 2-positive cancer. Clin Cancer Res 2011;**17**:6437-47.
31. Burris H, Rugo H, Vukelja S, Vogel C, Borson R, Limentani S, et al. Phase II study of the antibody drug conjugate trastuzumab-DM1 for the treatment of human epidermal growth factor receptor 2 (HER2)-positive breast cancer after prior HER2-directed therapy. J Clin Oncol 2011;**29**:398-405.
32. Barok M, Isola J, Palyi-Krekk Z, Nagy P, Juhasz I, Vereb G, et al. Trastuzumab causes antibody-dependent cellular cytotoxicity-mediated growth inhibition of submacroscopic JIMT-1 breast cancer xenografts despite intrinsic drug resistance. Mol Cancer Ther 2007;**6**:2065-72.
33. Bodyak N, Yurkovetskiy Y, Dmitry R. Gumerov DR, Xiao D, Joshua D, et al. Optimization of lead antibody selection for XMT-1522, a novel, highly potent HER2-targeted antibody-drug conjugate. Cancer Res 2016;**76**(14 Suppl), (abstract 596).

Figure legends

Figure 1.

Effect of T-DM1 and XMT-1522 on the growth (A-G) and caspase activity (H, I) of breast cancer and gastric cancer cells lines. Cell growth rate was assessed with the AlamarBlue method and apoptosis with the Caspase-Glo 3/7 method.

Figure 2.

Effect of T-DM1 and XMT-1522 on the growth of RN-87 xenografts in SCID mice (A). On day 35 after tumor inoculation the T-DM1 treatment was switched to either XMT-1522 1 mg/kg or XMT-1522 3 mg/kg in a few mice, and PBS treatment to either XMT-1522 1 mg/kg, XMT-1522 3 mg/kg, or T-DM1. (B) The drug administration schedule.

Figure 3.

Effect of T-DM1 and XMT-1522 on the growth of JIMT-1 xenografts in SCID mice (A). The drug administration times are indicated with arrows below the X-axis. One tumor treated with XMT-1522 1 mg/kg started to grow after initial shrinkage and was re-treated with the higher dose of XMT-1522 from day 99 onwards (pink arrows). (B) Survival of mice in the four treatment groups since the date of tumor inoculation.

Figure 4

Effects of T-DM1 and XMT-1522 on the formation of JIMT-1 xenografts (A). On day 43 after tumor inoculation a few mice had the treatment switched from T-DM1 to XMT-1522 1 mg/kg or 3 mg/kg. (B) The drug administration schedule. Survival calculated since the date of tumor inoculation (C) or since day 43 (D).

Figure 5

XMT-1522 evokes apoptosis. More apoptotic cancer cells (arrows) were present in RN-87 tumors (B) and JIMT-1 tumors (D) treated with XMT-1522 than in those treated with T-DM1 (A, C). Many apoptotic cells were present in a JIMT-1 tumor that relapsed after being treated with the 1 mg/kg dose of XMT-1522 but was sensitive (s.) to the 3 mg/kg dose of XMT-1522 (E). Few apoptotic cells were present in the tumors that progressed first on T-DM1 then on XMT-1522 (r.) (F). The bar = 30 μm.

Figure 6

Potential resistance mechanisms to T-DM1. (A) Selected differentially expressed mRNAs in T-DM1 sensitive (N-87 and OE-19) and resistant (RN-87 and ROE-19) HER2-positive gastric cancer cell lines in a gene expression microarray. (B) Flow cytometric quantification of HER2 in seven cell lines. T-DM1-resistant RN-87 and ROE-19 cells had lower levels of HER2 compared to the T-DM1-sensitive N-87 and OE-19 cells (P = 0.005 and P = 0.007, respectively). (C) Associations between the drug responses (IC_{50} values) and the numbers of cell surface HER2 receptors. (D-F) Flow cytometric quantification of ABCC1, ABCC2, and ABCG2 expression in T-DM1-sensitive and T-DM1-resistant gastric cancer cell lines. ABCC1: N-87 vs. RN-87, P = 0.0030; OE-19 vs. ROE-19, P = 0.0059. ABCC2: N-87 vs. RN-87, P = 0.1872; OE-19 vs. ROE-19, P = 0.0038. ABCG2: N-87 vs. RN-87, P = 0.0013; OE-19 vs. ROE-19, P = 0.0184. (G-I) The effect of ABC transporter-inhibitors tetrandrine, MK571, and elacridar as single agents or in combination with T-DM1 in RN-87 (G, H) and ROE-19 (I) cells. The combination resulted in the lowest cell survival. T-DM1 vs. tetrandrine + T-DM1, P = 0.0017; T-DM1 vs. MK571 + T-DM1, P = 0.0023; T-DM1 vs. elacridar + T-DM1, P = 0.0001.

Fig. 1

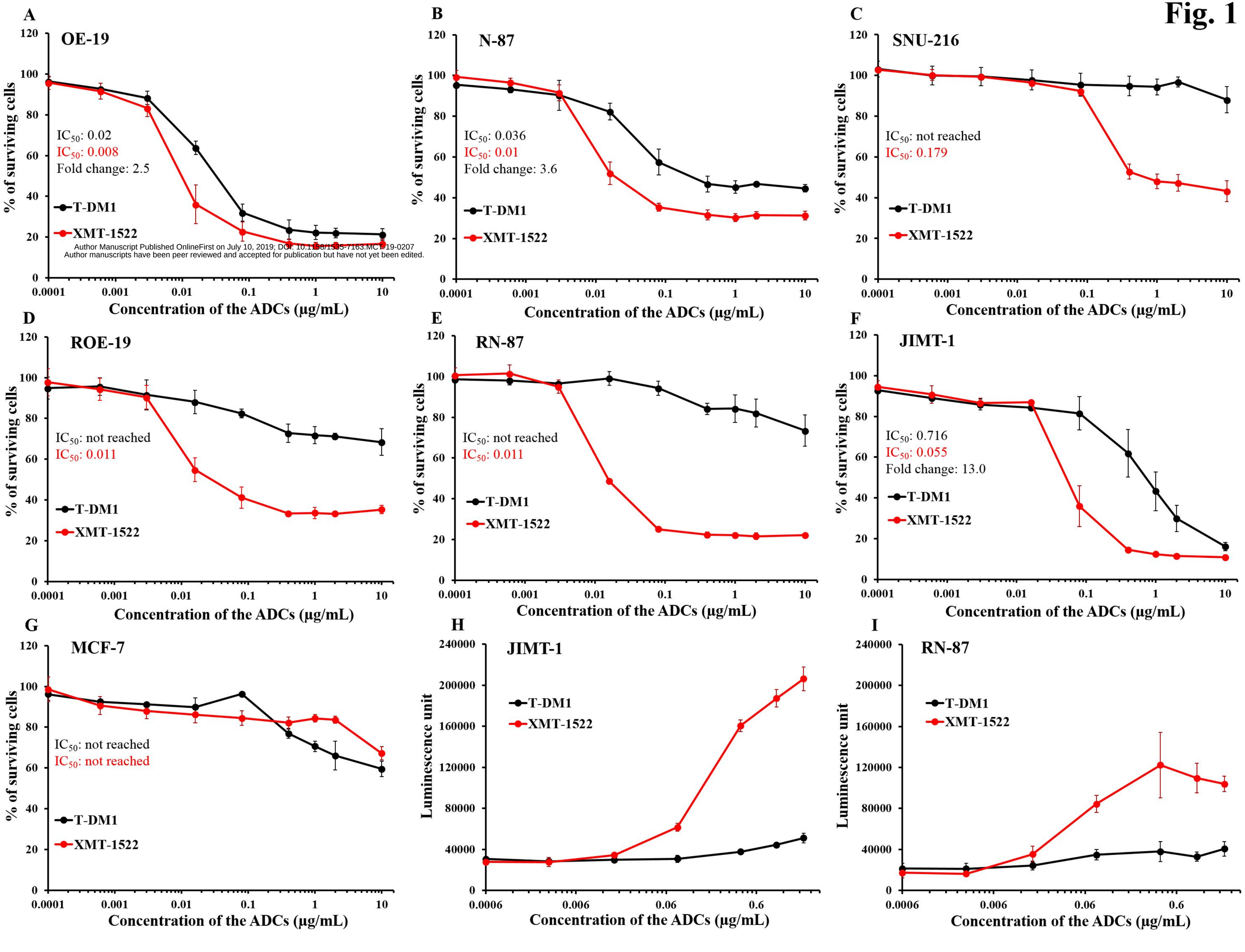

Author Manuscript Published OnlineFirst on July 10, 2019; DOI: 10.1158/1535-7163.MCT-19-0207
Author manuscripts have been peer reviewed and accepted for publication but have not yet been edited.

A

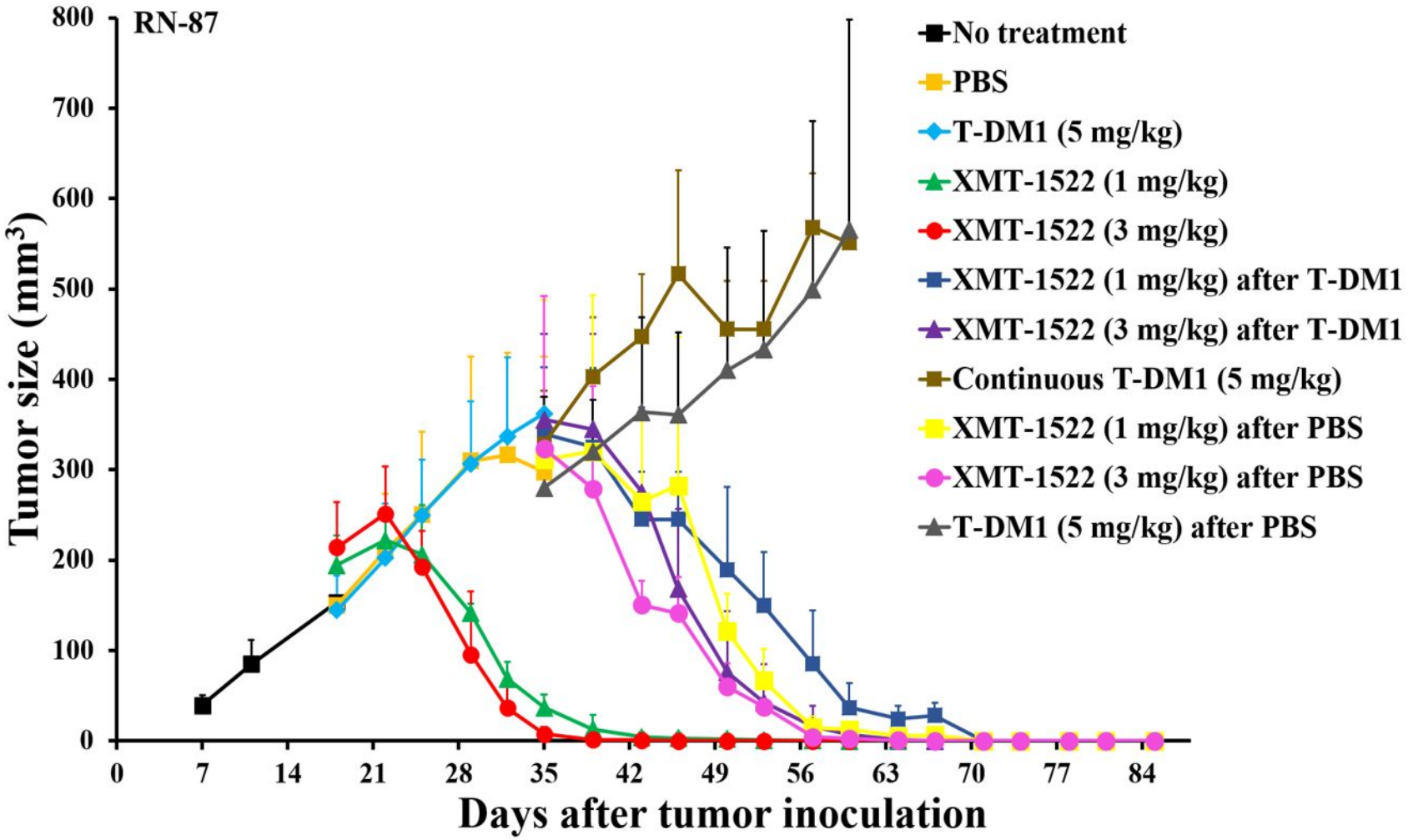

B

Drug administration schedule

Treatment group \ Treatment day	19	26	35	42	49	56	63	70	77	84
PBS	PBS	PBS								
T-DM1 (5 mg/kg)	T-DM1	T-DM1								
XMT-1522 (1 mg/kg)	XMT-1522	XMT-1522	XMT-1522		XMT-1522	XMT-1522	XMT-1522			
XMT-1522 (3 mg/kg)	XMT-1522	XMT-1522	XMT-1522							
XMT-1522 (1 mg/kg) a. T-DM1	T-DM1	T-DM1	XMT-1522	XMT-1522	XMT-1522	XMT-1522	XMT-1522			
XMT-1522 (3 mg/kg) a. T-DM1	T-DM1	T-DM1	XMT-1522	XMT-1522	XMT-1522					
Continuous T-DM1 (5 mg/kg)	T-DM1	T-DM1	T-DM1	T-DM1	T-DM1	T-DM1				
XMT-1522 (1 mg/kg) a. PBS	PBS	PBS	XMT-1522	XMT-1522	XMT-1522	XMT-1522	XMT-1522			
XMT-1522 (3 mg/kg) a. PBS	PBS	PBS	XMT-1522	XMT-1522	XMT-1522					
T-DM1 (5 mg/kg) a. PBS	PBS	PBS	T-DM1	T-DM1	T-DM1	T-DM1				

Fig. 3

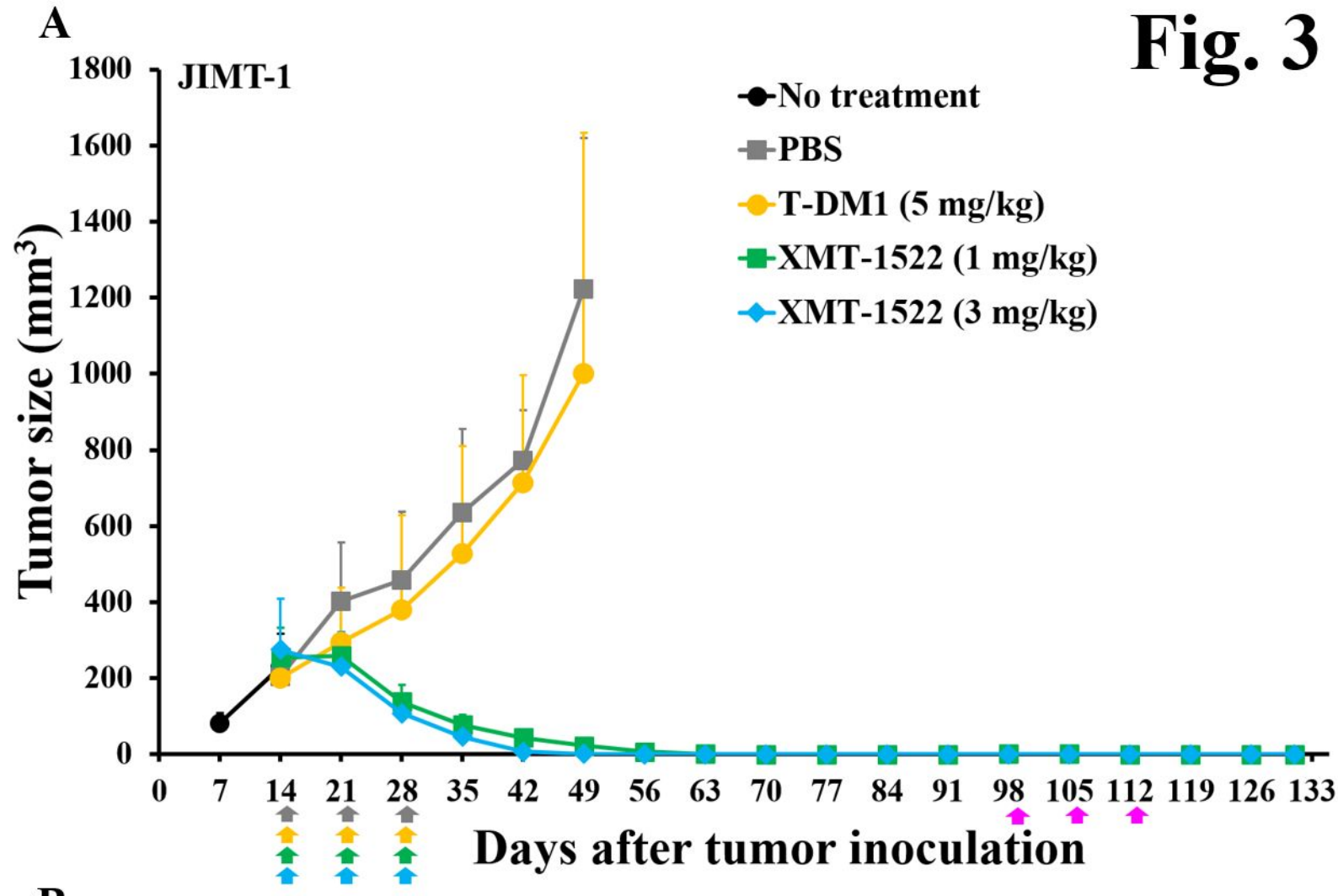

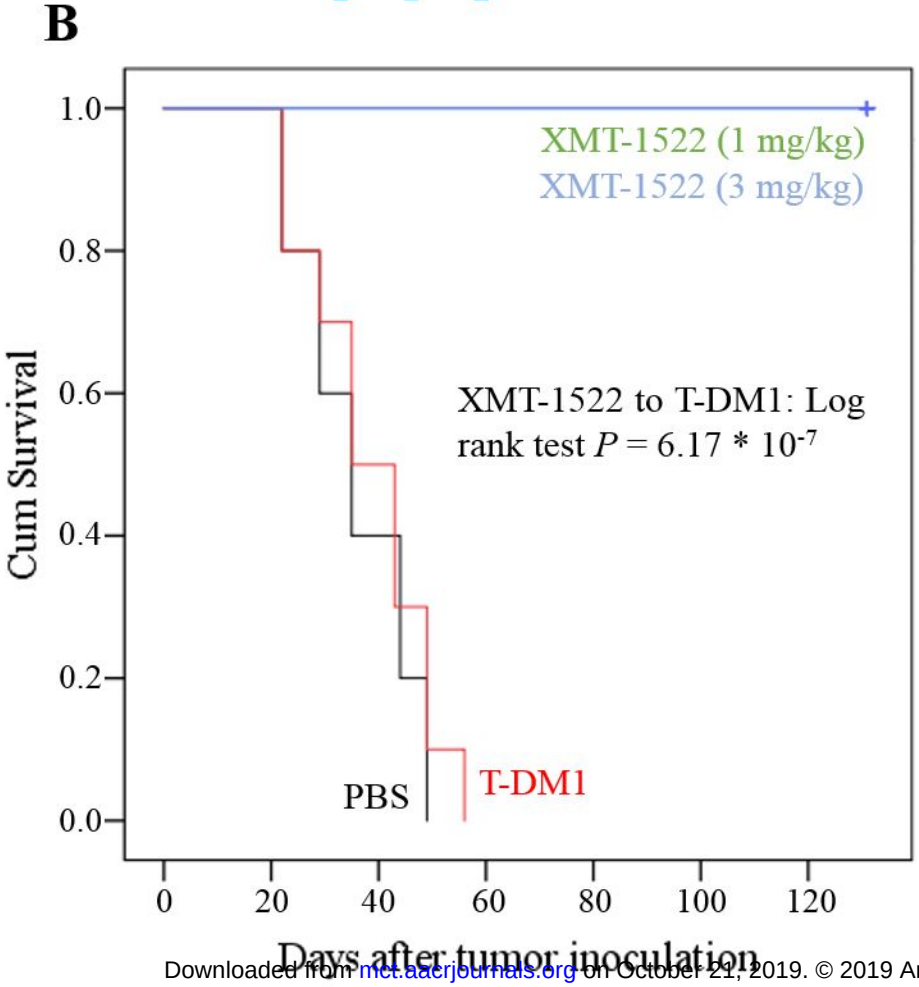

Fig. 4

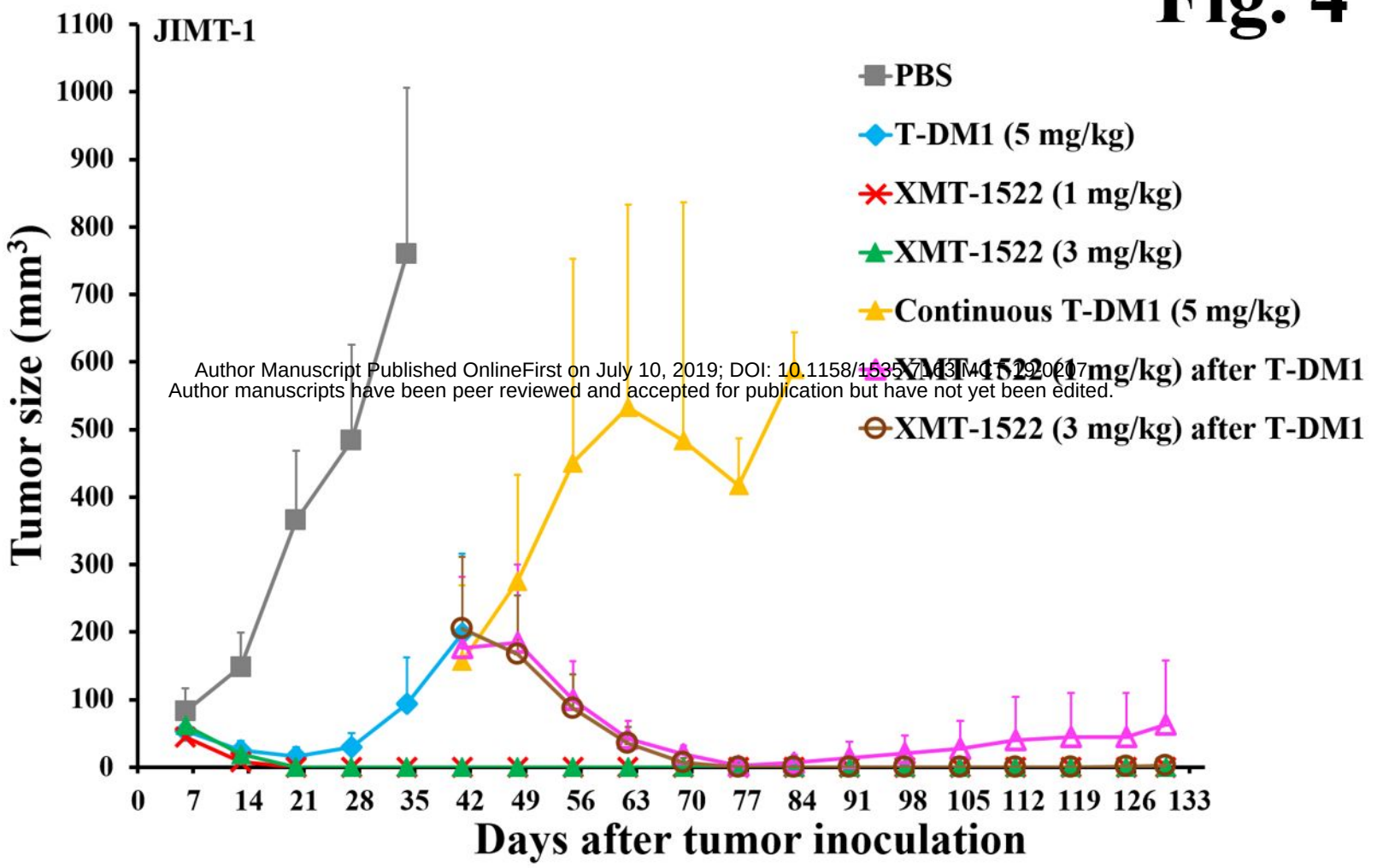

B Drug administration schedule

Treatment day / Treatment group	0	7	15	22	29	36	43	50	57	64	71	78	85	91	98	105	112	119	126	133
PBS	PBS	PBS	PBS	PBS	PBS															
T-DM1	T-DM1	T-DM1	T-DM1	T-DM1	T-DM1	T-DM1														
XMT (1 mg/kg)	XMT	XMT	XMT	XMT	XMT	XMT														
XMT (3 mg/kg)	XMT	XMT	XMT																	
Cont. T-DM1	T-DM1	T-DM1	T-DM1	T-DM1	T-DM1	T-DM1	T-DM1	T-DM1	T-DM1	T-DM1	T-DM1	T-DM1								
XMT (1 mg/kg) a. T-DM1	T-DM1	T-DM1	T-DM1	T-DM1	T-DM1	T-DM1	XMT	XMT	XMT					XMT	XMT	XMT	XMT			
XMT (3 mg/kg) a. T-DM1	T-DM1	T-DM1	T-DM1	T-DM1	T-DM1	T-DM1	XMT	XMT	XMT											

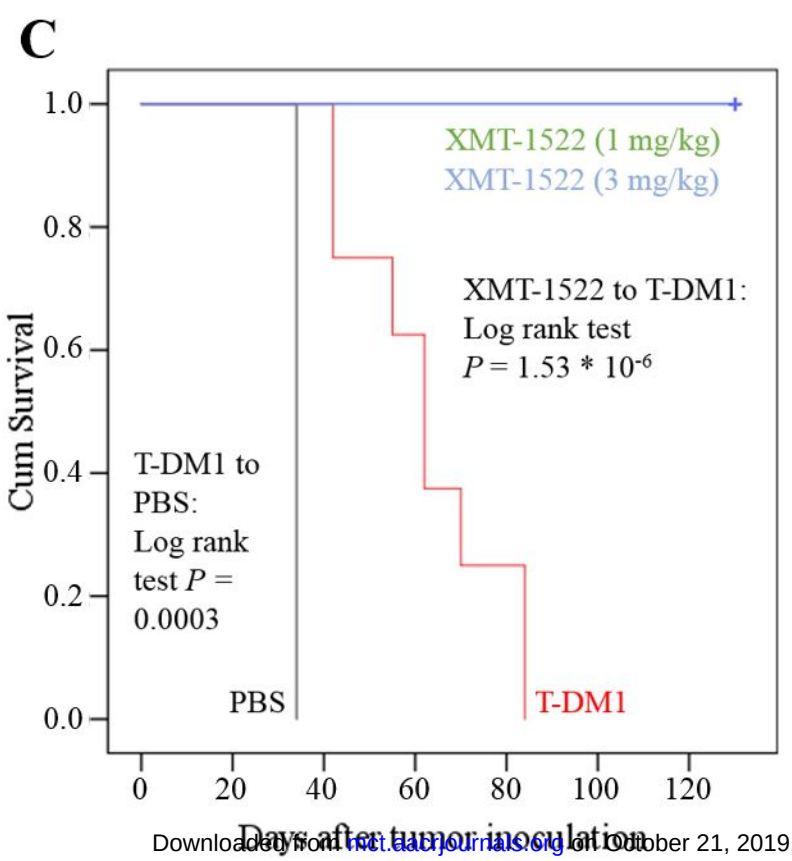

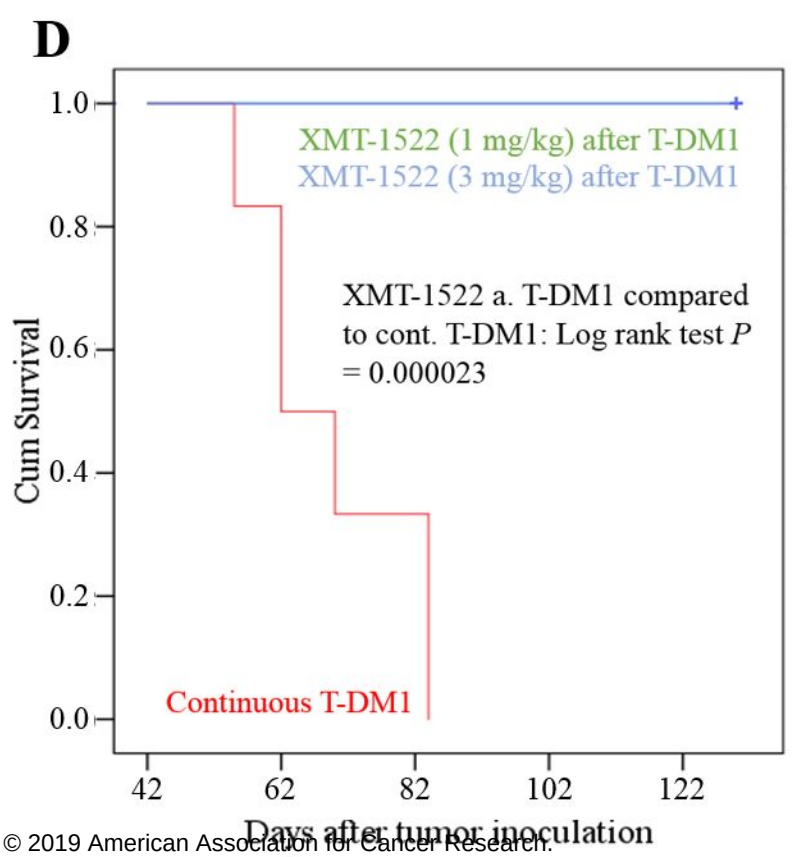

Fig. 5

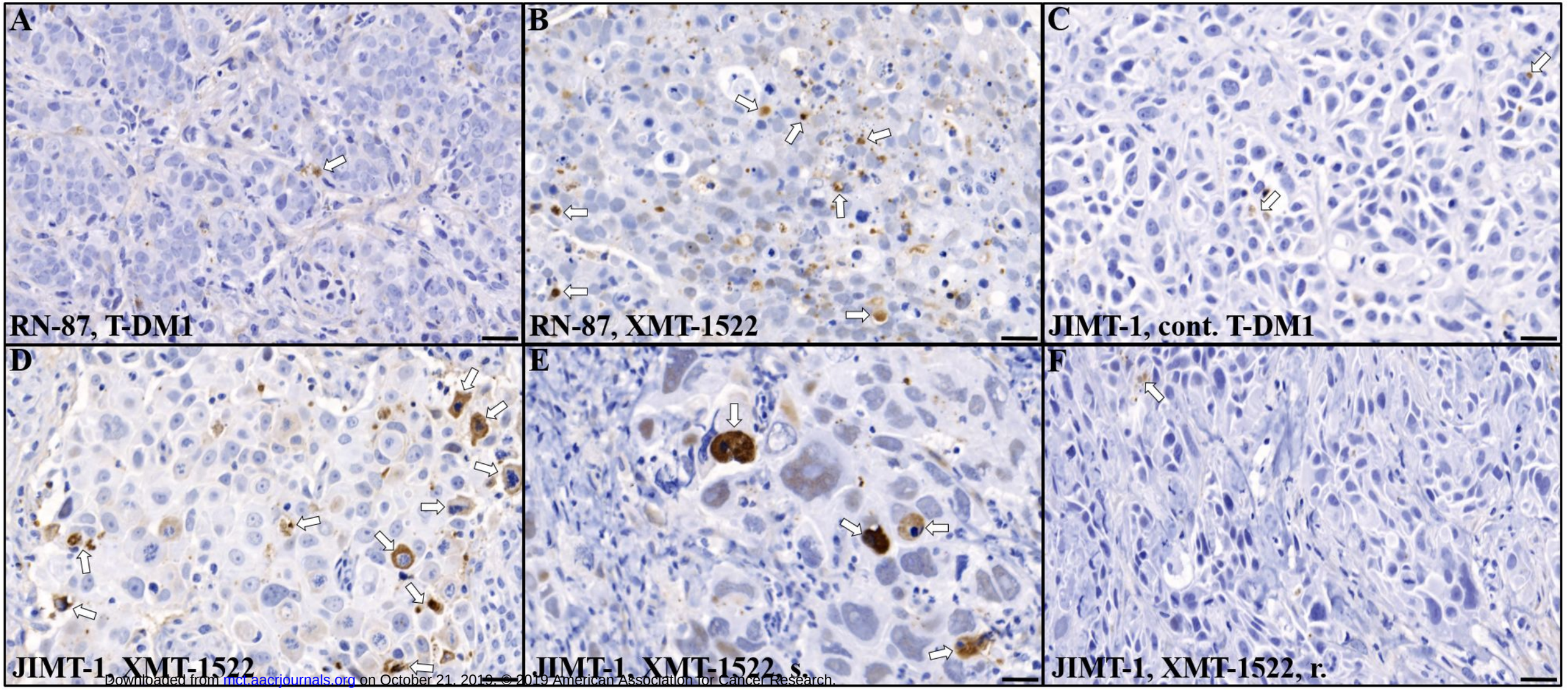

Fig. 6

A

Gene	RN-87 vs. N-87		ROE-19 vs. OE-19	
	Fold change	P-value	Fold change	P-value
ERBB2	-1.35	$2.23 * 10^{-2}$	-1.72	$2.7 * 10^{-3}$
ABCC1	3.34	$8.48 * 10^{-6}$	97.92	$1.01 * 10^{-12}$
ABCC2	1385.45	$1.9 * 10^{-10}$	37.39	$1.42 * 10^{-9}$
ABCG2	116.16	$1.98 * 10^{-10}$	9.25	$4.1 * 10^{-8}$

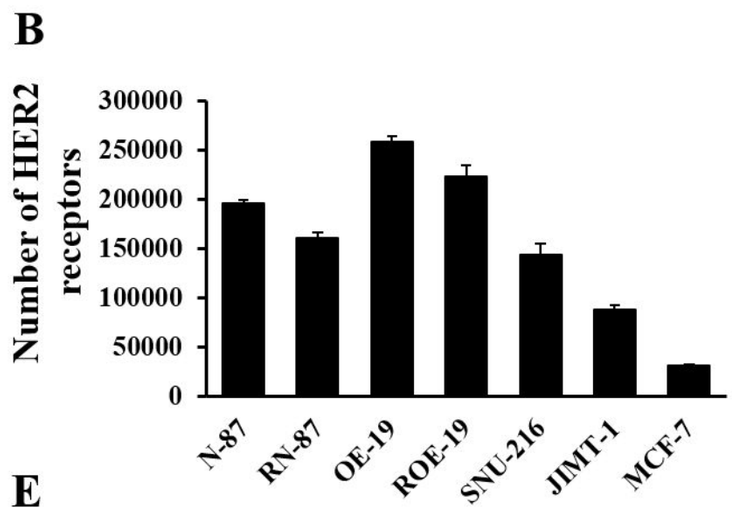

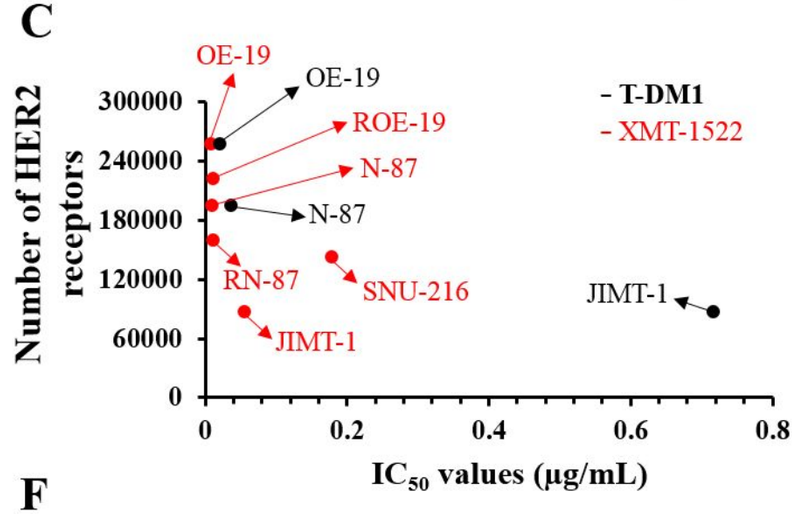

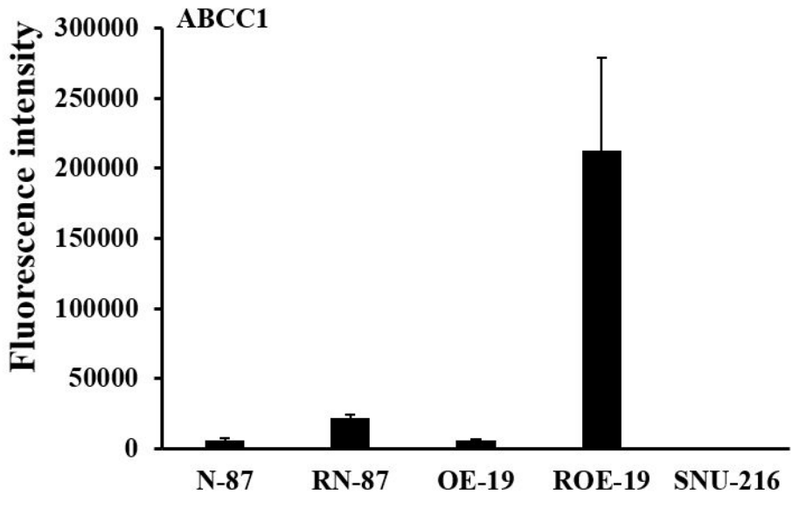

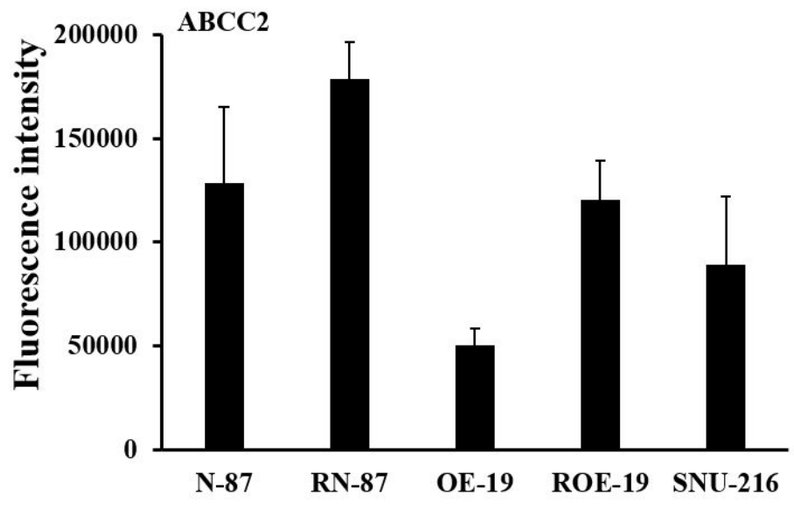

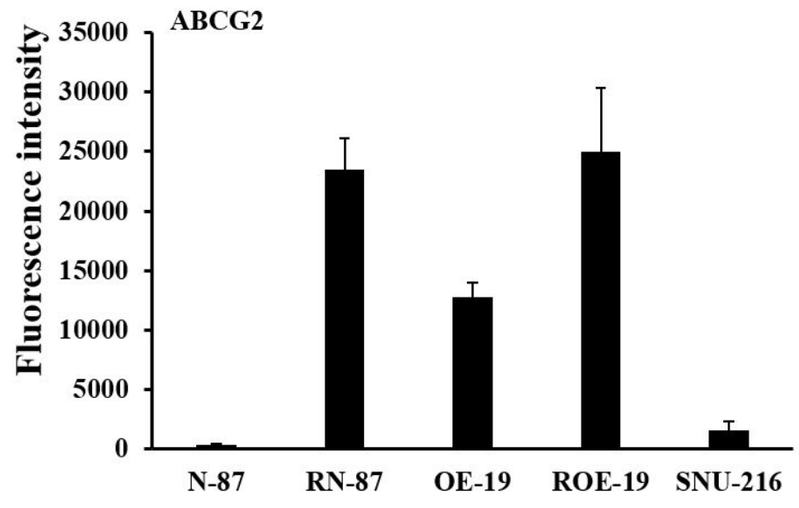

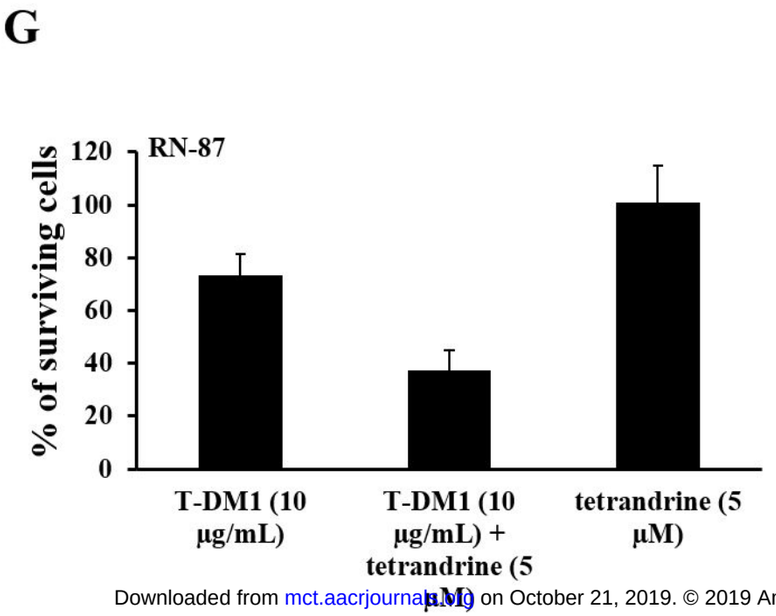

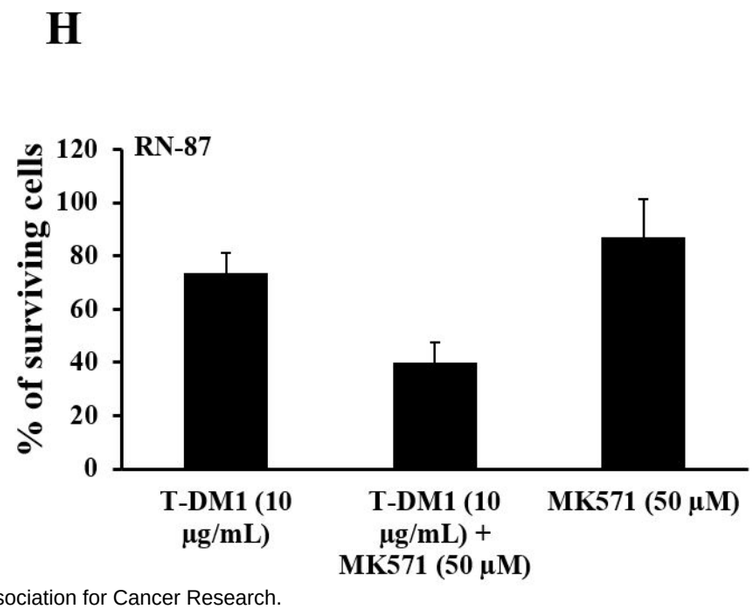

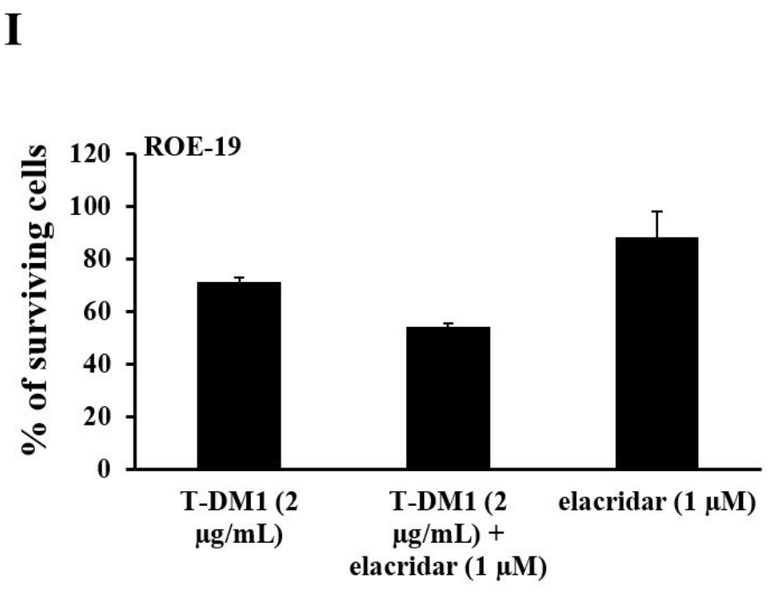

AACR American Association for Cancer Research

Molecular Cancer Therapeutics

A Novel Anti-HER2 Antibody-Drug Conjugate XMT-1522 for HER2-Positive Breast And Gastric Cancers Resistant to Trastuzumab Emtansine

Vadim Le Joncour, Ana Martins, Maija Puhka, et al.

Mol Cancer Ther Published OnlineFirst July 10, 2019.